

Properties of Rigid Polyurethane Foams Prepared from Recycled Aircraft Deicing Agent with Hexamethylene Diisocyanate

Bao Wang,^{1,2} Yan-Ling Cheng,^{1,3} Yuhuan Liu,^{1,4} Paul Chen,¹ Dong Li,² Roger Ruan¹

¹Center for Biorefining and Department of Bioproducts and Biosystems Engineering, University of Minnesota, St. Paul, Minnesota 55108

²Department of Agricultural Engineering, College of Engineering, China Agricultural University, Beijing 100083, China

³Department of Biological Medicine, College of Biochemical Engineering, Beijing Union University, Beijing 100023, China

⁴Biomass Energy Center and State Key Laboratory of Food Science, Nanchang University, Jiangxi 330047, China

Correspondence to: R. Ruan (E-mail: ruanx001@umn.edu)

ABSTRACT: Polyurethane (PUR) rigid foams were prepared from recycled aircraft deicing agent (aircraft deicing fluid) with reaction of hexamethylene diisocyanate at temperature of 55°C. The effect of [NCO]/[OH] ratio on properties of microscopic structure, cell size distribution, compressive strength, apparent density, as well as thermal conductivity (*k*) was studied. Higher [NCO]/[OH] ratio helped achieve better micro-morphology, higher apparent density, and compressive strength of the PUR foams. With the [NCO]/[OH] ratio of 0.75 and 0.8, some shrinking happened during foam rising, causing a decrease in total volume of the PUR foam, and leading to higher apparent density as well as sharply increased compressive strength. All PUR foams displayed good thermal insulation properties in this study. With [NCO]/[OH] ratio increased from 0.7 to 0.8, the *k* value increased significantly from 34.3 to 42.2 mW m⁻¹ K⁻¹. The *k* value here was chiefly governed by the apparent density of the foams, which was in turn a function of the ratio of [NCO]/[OH]. © 2012 Wiley Periodicals, Inc. *J. Appl. Polym. Sci.* 000: 000–000, 2012

KEYWORDS: compression; foams; microstructure; polyurethanes; thermal conductivity

Received 4 October 2011; accepted 19 February 2012; published online

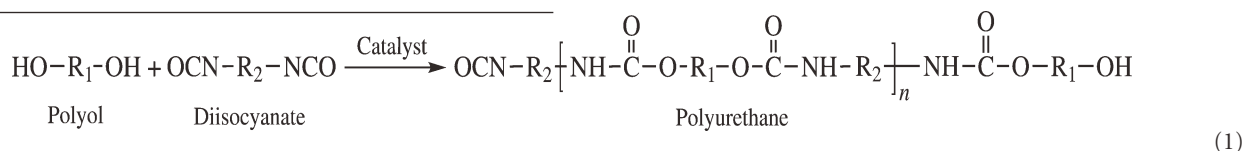
DOI: 10.1002/app.37525

INTRODUCTION

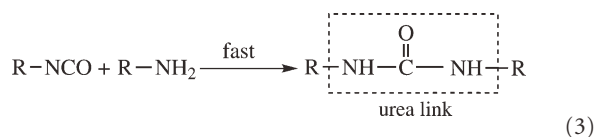
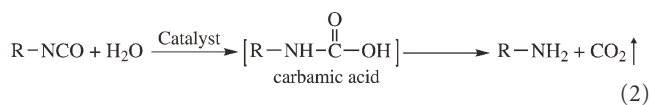
Polyurethane (PUR) rigid foam is one of the most important thermal insulating materials used in constructions and other areas. The PUR foam works more effectively than fiberglass in thermal insulation.¹ Nowadays, PUR foams are generally produced by polymerization of polyols/diols and isocyanates, both of which are produced mostly from petroleum-based products.² Due to the increasing consumption as well as limited availability of fossil resources, many researchers are seeking alternative raw materials for oil-based polyols, such as bio-based polyols from vegetable oils, including soybean oil, castor oil, rape oil, linseed oil, safflower oil, and palm oil^{3–5} or from biomasses such as stover, wood, and dried distiller grains.^{1,6,7}

During the formation of the PUR foam, generally two kinds of reactions take place. One reaction is between isocyanate and

polyol/diol, which produces urethane links (—NH(CO)O—) and polymerizes PUR [as shown in Eq. (1)]. Another reaction is between isocyanate and water, which can be divided into two steps, and the reaction equations are given in eqs. (2) and (3). As shown in Eq. (2), water first reacts with isocyanate and produces a carbamic acid, which is very unstable and quickly decomposes into amine and carbon dioxide (appears as foam bubbles). Then quickly the amine from Eq. (2) reacts with isocyanate and produces urea links [Eq. (3)]. Therefore, the two kinds of reactions cause an increase in apparent viscosity and form the cross-linking framework of the PUR foam subsequently. Due to increase in the apparent viscosity of the mixed reaction agents, a lot of the carbon dioxide diffuses into the “solution,” which then helps form the cell structures and causes the foam to rise.



© 2012 Wiley Periodicals, Inc.



Every year, large quantities of aircraft deicing and anti-icing fluids (ADFs and AAFs) containing propylene glycol (PG) and ethylene glycol (EG) are used in airports. The spent deicing/anti-icing agents containing water have to be collected and disposed, which actually becomes a big problem. The main concern regarding the environment impacts of such ADF-/AAF-containing wastewater focuses on the oxygen consumption during the decomposition of the deicing materials.⁸ Polyols in deicing agent have a high biochemical oxygen demand (BOD) level. For example, it is reported that pure EG has a BOD₅ (BOD for 5 days) value of 400,000–800,000 mg L⁻¹, whereas pure PG has such a value of 1,000,000 mg L⁻¹.⁹ Therefore, if the ADFs/AAF containing runoff was directly discharged into the receiving waters, it would cause a decrease in the available oxygen that would impact aquatic life.

Currently, there are several methods to treat such ADFs/AAF containing wastewater. One method is to treat and dispose such an effluent by aerobic or anaerobic treatment. After these treatments, the polyols/diols can be almost completely destroyed, and the BOD concentration can be decreased significantly. However, generally the capital cost for such processes is very high. Another way is to recycle the glycols from the ADF-/AAF-containing runoff. Recycling systems rely on a series of standard separation techniques to remove water, suspended solids, as well as other surfactants and corrosion inhibitors from the wastewater.⁸ After the recycling process, typical products from evaporation-based systems (using evaporation to remove water) contain about 50–60% glycols.¹⁰ The recovered glycols are normally reprocessed and sold for use in nonaircraft applications, which are used as drilling fluids, automobile antifreeze, or industrial coolants. However, if the recycled ADF/AAF containing polyols/diols is used to produce PUR foams, it can not only help eliminate the potential pollution to the environment but also help reduce the consumption of fossil materials.

The objective of this study was to explore the possibility of making PUR foams using recycled ADF. The [NCO]/[OH] ratio is a very important parameter to control the quality of the PUR foams. With the variation of this ratio, the properties of the PUR foams can be controlled effectively.⁶ In this study, the recycled ADF was directly used in the preparation of PUR rigid foams. Cell morphology analysis, compressive strength, apparent density, as well as thermal insulation property of the PUR foams were characterized, and the effect of [NCO]/[OH] ratio on foam quality was evaluated.

Table I. Composition of the PUR Foams with Different [NCO]/[OH] Ratios

[NCO]/[OH]	Used				
	deicing agent (g)	Glycerin (g)	HDI (g)	Silicon oil (g)	Stannous octoate (g)
0.4	5.0	2.5	14.8	1.0	0.8
0.5	4.0	2.0	14.8	0.8	0.9
0.6	4.0	2.0	17.8	0.8	1.0
0.7	4.0	2.0	20.7	0.8	1.1
0.75	4.0	2.0	22.2	0.8	1.2
0.8	4.0	2.0	23.7	0.8	1.2

MATERIALS AND METHODS

Materials

Recycled ADF was provided by John F. Kennedy (JFK) International Airport located in New York. The recycled ADF, as a mixture of propylene glycol and water, contains 48.4 wt % (weight percent) propylene glycol and 51.6 wt % water. The composition information was provided by the JFK airport, and the moisture content was validated in our lab using an automatic Karl Fisher titrator (TitroLine, Schott Instruments, White Plains, New York). Hexamethylene diisocyanate (HDI) (>98.0%), stannous octoate (about 95%), silicon oil, and glycerin were purchased from Sigma-Aldrich.

Preparation of Rigid PUR Foam

A homebuilt reactor was used to produce PUR rigid foams in this study. A water bath beaker was held on the top of a magnetic stirring heater with a temperature of 55.0°C. Known amounts of recycled ADF, silicon oil, glycerin, and stannous octoate were added into a medium-size paper cup. Glycerin acted as a cross-linking agent. Water contained in the recycled ADF was used directly as a blowing agent, stannous octoate as a catalyst, whereas silicon oil was used as a stabilizer. After initial mixing, the paper cup was placed inside the water bath beaker and was stirred by the magnetic stirrer with a mixing rate of 400 rpm for 2 min 30 s. Then, a designated amount of HDI was slowly added to the mixed liquid, while the mixing rate was kept constant. The mixing was stopped when some bubbles appeared, which usually lasted 1–2 min. When the foaming process was completed, the PUR foam samples were cured at room temperature (around 25.0°C) for at least 3 days before tests. Each sample was prepared in five replicates, and the typical PUR foam formula is listed in Table I. The components in Table I as well as all other processing parameters in this report were all chosen based on our preliminary studies.

As the reaction agents are low molecular compounds with clear composition and molecular formula, the hydroxyl group (—OH) number can be calculated directly as follows:

$$N = m \cdot f / M, \quad (4)$$

where N is the group number of —OH, m is the mass of the reaction agent (g), f is the number of reactive groups inside a molecule, and M is the molar mass of the reaction agent (g mol⁻¹).

As a result, the [NCO]/[OH] ratios of the PUR foams were calculated as follows:

$$\frac{[\text{NCO}]}{[\text{OH}]} = \frac{m_{\text{iso}} \times K_{\text{iso}}}{m_{\text{PG}} \times 2/76.09 + m_{\text{glycerine}} \times 3/92.09 + m_{\text{water}} \times 2/18}, \quad (5)$$

where K_{iso} is the content of [NCO] in 1 g on HDI (about $0.0117 \text{ mol g}^{-1}$), while m_{iso} , m_{PG} , $m_{\text{glycerine}}$, and m_{water} are the masses (g) of HDI, propylene glycol, glycerin, and water, respectively. In this study, the range of [NCO]/[OH] ratio used was from 0.4 to 0.8. For simplicity, PUR foams with [NCO]/[OH] ratio of 0.4, 0.5, 0.6, 0.7, 0.75, and 0.8 were designated as Samples A–F, respectively.

Microscopic Study of the HMS Dispersions

To investigate the cell morphology of the foams with different [NCO]/[OH] ratios, all samples were examined using an optical microscope (DC5-163 Digital Microscope, National Optical & Scientific Instruments Inc., San Antonio, Texas). The microscope was equipped with a CCD camera, and the software of “Motic Images Plus 2.0” was used to take micrographs. The PUR foams were cut into slices, and the cellular structure of the foams was observed parallel to the foam rising direction.

Cell size analysis was conducted using the software of ImageJ. The scale was preset by measuring the standard length produced from a digital caliper. Several different methods can be used to calculate the diameter of the cells, while in this study the apparent long axis (i.e., maximum diameter inside a cell) was collected for analysis. In this study, 200–260 cells were measured for each sample.

Compressive Strength of the Foams

Mechanical properties of the PUR foams were tested in accordance with American Society of Testing and Materials (ASTM) procedure D1621-04a. The compressive strength (σ_c) was measured using an Instron testing machine (Instron-4206, Instron, Norwood, Massachusetts) at room temperature (around 25.0°C). The foams to be tested were cut into cylinders with a size of 26.0 mm in thickness and 63.0 mm in diameter. The crosshead speed was set at 2.5 mm min^{-1} , and the samples were compressed in the direction parallel to the free rising direction. The load was applied, until the foam was compressed to $\sim 50\%$ of its original thickness.

The compressive strength was defined as the stress at 10% deformation of the original thickness. When the yield point occurred before 10% deformation, the compressive strength was obtained at the yield point. Five parallel tests were done for each sample.

Apparent Density of PUR Foams

The apparent density of the PUR foam was calculated according to ASTM D 1622-03. Triplicate parallel tests were done for each sample.

Thermal Insulation Properties of the Foams

Thermal conductivity (k) of the PUR foams was tested using KD-2 Thermal Properties Analyzer (Decagon Devices, Pullman, Washington). The KD-2 analyzer has a probe with length of 60.0 mm and diameter of 0.9 mm, which measures the k value through monitoring the dissipation of heat from a line heat source. After the probe was inserted into the foam, the analyzer showed directly the k value in 2 min. For any sample measurement, the probe was inserted and kept parallel to the direction of foam rising. Five replicates were conducted for each sample.

Statistical Analysis

Parallel tests were carried out for all the experiments described before, means and standard deviations of each experiment were presented for the data. A one-way analysis of variance and Tukey's test were used to establish the significance of differences among the mean values at the 0.95 level of confidence. The statistical analysis was performed using SPSS (2003) version 13.0 for Windows program (SPSS, Chicago, Illinois).

RESULTS

Micrographs of the PUR Foams

The micrographs of the PUR foams made from recycled ADF are shown in Figure 1. From Figure 1, the microscopic morphology and cell size changed obviously with the increase in [NCO]/[OH] ratio. At the [NCO]/[OH] ratio of 0.4 [Figure 1(A)], the cells were larger than at other ratios, and small cells were merely visible. However, with the ratio being increased from 0.5 to 0.8, generally the cell sizes decreased greatly, and foam structure appeared to be more uniform.

As indicated in the “Introduction” section, generally two kinds of reactions take place. One reaction is between HDI and PG/glycerin, which produces urethane links ($-\text{NH}(\text{CO})\text{O}-$) and polymerizes PUR [as shown in Eq. (1)]. Another reaction is between HDI and water, which can be divided into two steps, and the reaction equations are given in eqs. (2) and (3). It is reported that the reaction rate between isocyanate and water is greater than that between isocyanate and polyols/diols.¹¹ Besides, it should be noted that the molar concentration of water is about 2.4 times higher than the total molar concentration of both PG and glycerin. As a result, it is reasonable to estimate that HDI would react with water first. Therefore, with [NCO]/[OH] ratio of 0.4, more HDI reacted with water first, whereas the reaction between HDI and PG/glycerin was weak and slow. Such a reaction characteristic destroyed the balance between the two reactions, resulting in the quick release of most carbon dioxide into environment. Though some carbon dioxide was sequestered into the foam, generally the cells were very large due to relatively low viscosity of the mixture during CO_2 releasing.

With the increase in [NCO]/[OH], balance between the two reactions can be better achieved. Generally, the cell size decreased with increasing [NCO]/[OH] ratio. As it can be observed from Figure 1(E,F), the cell sizes of Samples E and F become smaller and more uniform, indicating that better foam structures can be reached with [NCO]/[OH] ratios of 0.75 and 0.80.

Morphology Analysis of the PUR Foams

Cell size is a parameter important to both mechanical and thermal insulation properties of the rigid PUR foams. To better understand the effect of [NCO]/[OH] ratio on micromorphology of the PUR foams, cell size analysis was performed using ImageJ. The cell size distribution of the PUR foams is displayed in Figure 2, whereas the data summary is given in Table II.

From Figure 2(A,B), it can be observed that samples with lower [NCO]/[OH] ratios (0.4 and 0.5) tend to have a broader size distribution. For the PUR foams with the [NCO]/[OH] ratio of

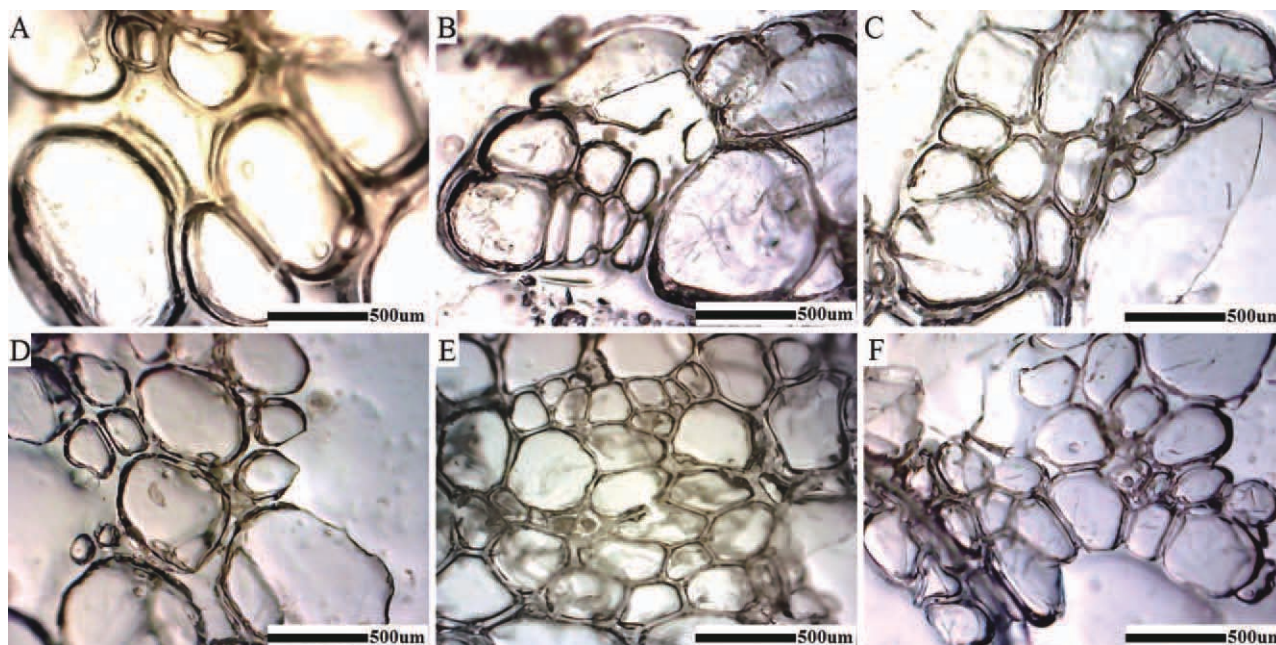


Figure 1. Microstructure of the PUR foams produced with different [NCO]/[OH] ratios: (A) ratio = 0.4; (B) ratio = 0.5; (C) ratio = 0.6; (D) ratio = 0.7; (E) ratio = 0.75; and (F) ratio = 0.8. [Color figure can be viewed in the online issue, which is available at wileyonlinelibrary.com.]

0.4–0.5, though the majority of the cells have sizes within lower range (0–700 nm), disorderly distribution pattern was displayed in general. Compared with Samples A and B, the average cell size and standard deviation of Sample C decreased a lot (from 0.724 ± 0.435 mm for Sample A and 0.604 ± 0.414 mm for Sample B, to 0.43 ± 0.276 mm for Sample C). Furthermore, the ratio for cell size among 0–700 nm of Sample C also increased significantly compared with Samples A and B (from 57.5% and 64.4% for Samples A and B to 82.2% for Sample C). Such results indicate that the micromorphology became much better with [NCO]/[OH] ratio being increased to 0.6.

With the [NCO]/[OH] ratios of 0.7, 0.75, and 0.8, the size distribution of Samples D–F appeared to be more orderly with smaller average cell sizes as well as smaller standard deviations than Samples A–C (0.316 ± 0.209 mm, 0.247 ± 0.147 mm, and 0.334 ± 0.191 mm for Samples D–F, respectively). In all the foam samples, Sample E with [NCO]/[OH] ratio of 0.75 displayed best cell size distribution for the smallest values of average cell size and standard deviation, as well as largest value of “Ratio₇₀₀” (Table II). Such a result indicates that micromorphology of the samples in this study was not a monotone function of the [NCO]/[OH] ratio. In fact, cell size of the samples here depended on several factors such as balance of the reactions, apparent viscosity during CO₂ releasing, and pressure inside the bubbles. However, all these reaction conditions can be changed, and thus, the micromorphology of the PUR foams can be adjusted effectively through controlling [NCO]/[OH] ratio.

Mechanical Properties of the PUR Foams

Compressive strength of the samples was given in Figure 3. From Figure 3, the compressive strength generally exhibits a rising trend with increasing [NCO]/[OH] ratio. With the [NCO]/

[OH] ratio from 0.4 to 0.7, the samples (A–D) showed compressive strengths of 32.7 ± 10.2 , 30.8 ± 10.8 , 68.0 ± 9.5 , and 83.1 ± 17.1 kPa, respectively. However, with the [NCO]/[OH] ratio of 0.75 and 0.8, compressive strength of the PUR foams (Samples E and F) increased significantly compared with other samples ($P \leq 0.05$). The compressive strength of Samples E and F was 295.3 ± 66.3 and 375.5 ± 112.48 kPa, respectively, which was even better than the commercial PUR rigid foams.

It is reported that variation in the [NCO]/[OH] ratio can change the mechanical properties of PUR foams effectively.⁶ As a cross-linked material, the hardness of PUR foams is closely associated with the formation of cross-linked structures as well as hard segments. With the increase in [NCO]/[OH] ratio, the cross-linking degree and the hard segment of the PUR foam increased distinctly, through the reaction between HDI and PG/glycerin/water, which caused the increase in compressive strength of the PUR foams.¹² In this study, the increased [NCO]/[OH] ratio also produced better micromorphology with more uniform cell size, as indicated in “Micrographs of the PUR foams” and “Morphology analysis of the PUR foams” sections. Obviously, such better microscopic structure would help to enhance the mechanical properties effectively, which was in accordance with the stronger compressive strength of the PUR foams with higher [NCO]/[OH] ratios.

However, the above arguments are insufficient to explain the sharp increase in compressive strength for Samples E and F. It is assumed that such a sharp increase in compressive strength should be related to the foam rising process. For Samples A–D, the foam rising process was swift and stable, with foam volume increased directly to the maximum value. In general, the volume of the foam increased to a larger size with increasing [NCO]/[OH] ratio from 0.4 to 0.7. This phenomenon agrees with the

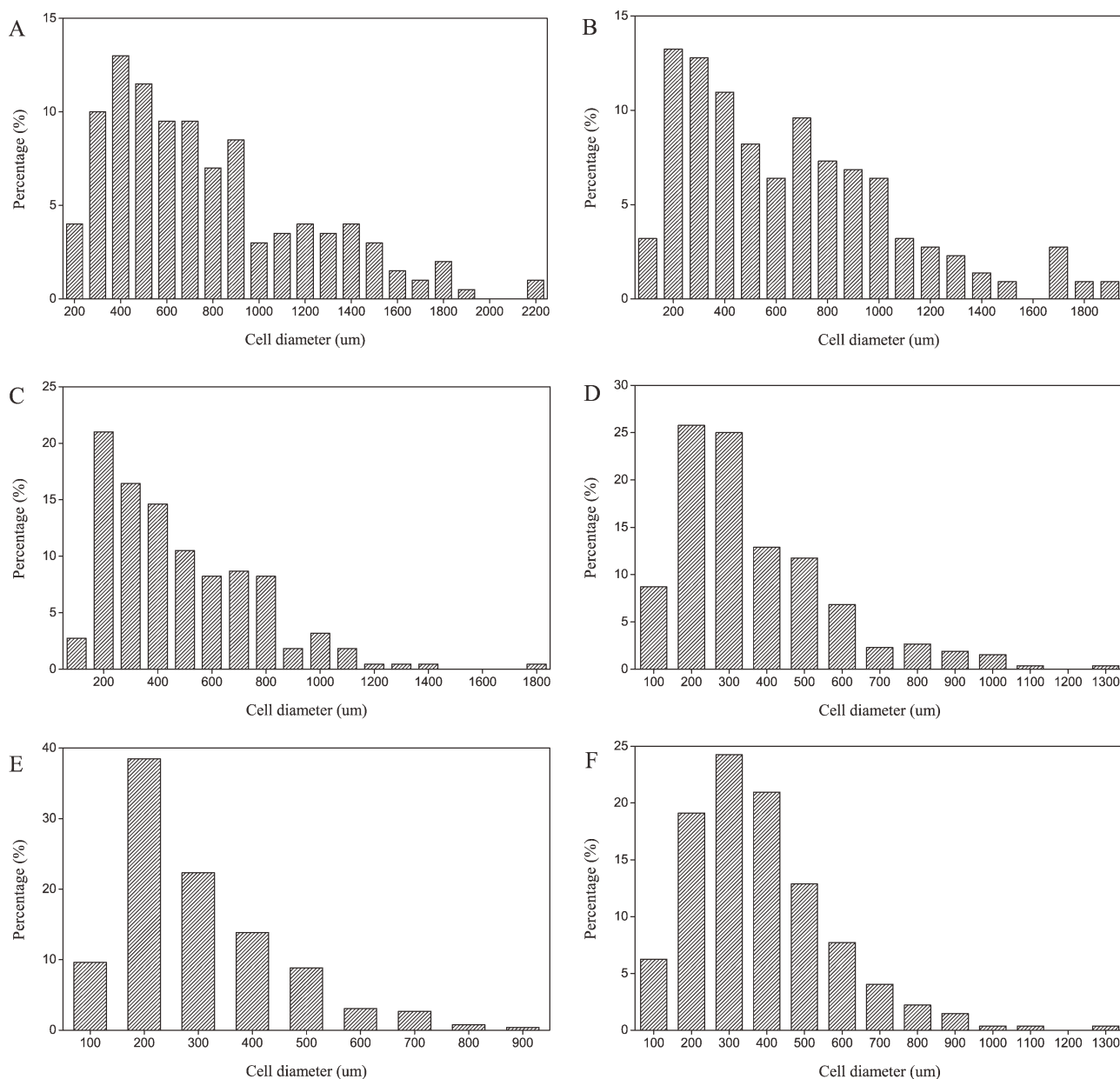


Figure 2. Cell size distribution of the PUR foams produced with different $[\text{NCO}]/[\text{OH}]$ ratios: (A) ratio = 0.4; (B) ratio = 0.5; (C) ratio = 0.6; (D) ratio = 0.7; (E) ratio = 0.75; and (F) ratio = 0.8.

apparent density of the samples. As can be observed in Figure 4, the apparent density decreased gradually with increasing $[\text{NCO}]/[\text{OH}]$ ratio from 0.4 to 0.7 (the apparent density was 71.6 ± 0.6 , 62.2 ± 4.6 , 62.2 ± 6.0 , and $59.5 \pm 4.0 \text{ kg m}^{-3}$ for Samples A–D, respectively). For these samples, the compressive strength increased with a smaller apparent density, indicating that a better foam structure could be achieved with an increase in $[\text{NCO}]/[\text{OH}]$ ratio from 0.4 to 0.7. However, the apparent density for Samples E and F increased significantly compared with Sample D ($P \leq 0.05$, 81.4 ± 9.8 and $89.6 \pm 6.7 \text{ kg m}^{-3}$ for Samples E and F, respectively). From observation of the reaction, the foam rising process was unstable for Samples E and F, because the reaction was more intensive with higher $[\text{NCO}]/[\text{OH}]$ ratios of 0.75 and 0.8. When the foam volume

increased to the maximum value, the structure of the PUR foam was not strong enough to hold sufficient carbon dioxide gas, which was quickly released from the reaction. Due to this reason, more carbon dioxide would escape, which then caused shrinking of the total volume. Also, more hard fragments and cross-linked structures could be formed with Samples E and F. When the foam rising reached the maximum volume, it is possible that the mass of PUR foam exceeded the load-bearing limit of the PUR structures, which then caused shrinkage. Such a contraction process led to increased apparent density of Samples E and F. Also, due to this contraction process, the foam structure was intensified significantly, which produced a stronger compressive strength. Sample F with higher ratio of $[\text{NCO}]/[\text{OH}]$ experienced a stronger contraction than Sample E, which

Table II. Summary of Cell Size from PUR Foams with Different [NCO]/[OH] Ratios

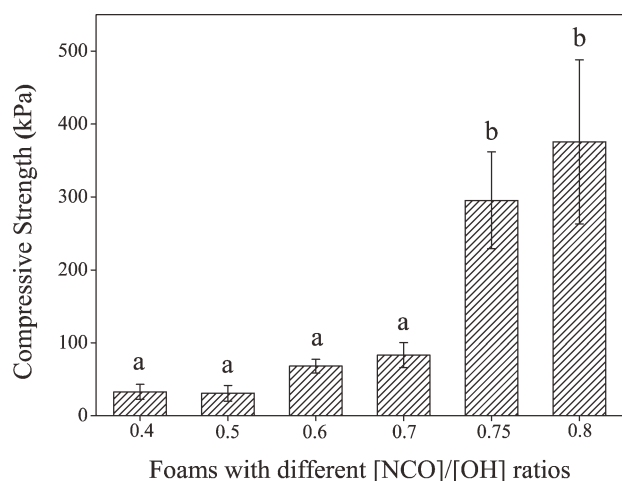
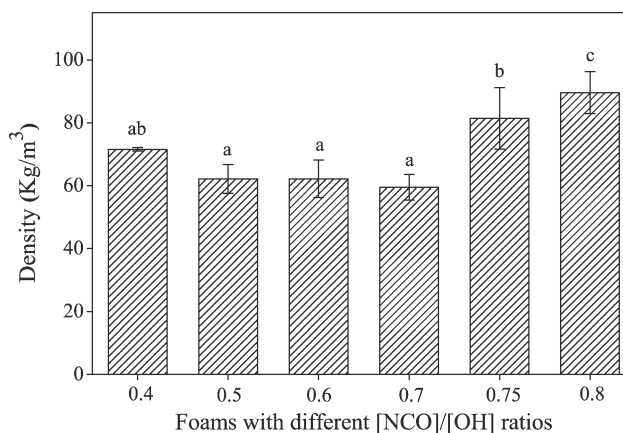
[NCO]/[OH]	Mean (mm)	SD (mm)	Min (mm)	Max (mm)	Ratio ₇₀₀ ^a (%)
0.40	0.724	0.435	0.132	2.159	57.5
0.50	0.604	0.414	0.059	1.823	64.4
0.60	0.43	0.276	0.049	1.718	82.2
0.70	0.316	0.209	0.035	1.255	93.2
0.75	0.247	0.147	0.042	0.826	98.8
0.80	0.334	0.191	0.038	1.261	95.2

Mean, mean size of cells; SD, standard deviation; Min, minimum value of the cell; Max, maximum value of the cell.

^aRatio₇₀₀ refers to percentage of the cells with diameters between 0 and 700 μm .

was in agreement with the greater apparent density and compressive strength of Sample F.

It can also be observed in Figure 3 that though Samples E and F displayed strong compressive strength during the mechanical tests, the standard deviation (which is also the absolute deviation) was large in value (66.3 and 112.5 kPa for E and F, respectively). Due to the swift foaming and contraction process as well as the quick cooling and curing, structure and apparent density of the foam were not uniform inside the cup. The PUR foam formed near the upper part of the cup has a stronger structure with higher apparent density, whereas the one formed near the bottom of the cup has a relatively weak structure with lower apparent density. Due to this nonuniformity at macro level, the PUR foams with NCO/OH ratio of 0.75 and 0.8 displayed a large deviation during mechanical tests. However, Samples A and B had even greater relative deviations than Samples E and F (the relative deviations were 31.2% and 35.2% for Samples A and B, whereas 20.5% and 22.4% for Samples E and F, respectively). Compared with other samples, Samples C and D had smaller relative deviations (14.0% and 20.5%, respectively),

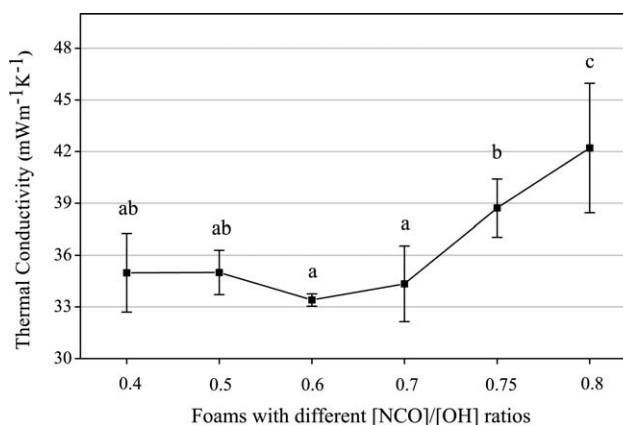
**Figure 3.** Compressive strength of the PUR foams produced with different [NCO]/[OH] ratios (data with different letters on the bar are significantly different, $P \leq 0.05$).**Figure 4.** Apparent density of the PUR foams made from recycled ADF with different [NCO]/[OH] ratios (data with different letters on the bar are significantly different, $P \leq 0.05$).

indicating better uniformity in mass distribution. Such results indicate that reactions were relatively unstable with larger (0.75 and 0.8) or smaller (0.4 and 0.5) [NCO]/[OH] ratios, whereas the reaction with [NCO]/[OH] ratio of 0.6 and 0.7 was more controllable.

Thermal Insulation Properties of the Foams

The PUR rigid foams are mainly used for thermal insulation in buildings and appliances. For this reason, thermal insulation is regarded as the most important property of the PUR rigid foams. The KD-2 thermal properties analyzer was commonly used in labs for testing thermal conductivities (k) of different materials, and the k values measured by KD-2 for our samples are given in Figure 5. Thermal conductivity refers to a material's ability to conduct heat, and a lower thermal conductivity value of the PUR foam indicates a better thermal insulation capability.

From Figure 5, all PUR foams showed a k value with a range of 33.4–41.8 $\text{mW m}^{-1} \text{K}^{-1}$. Such a range of k value was similar to those of expanded polystyrene (about 32.0–40.0 $\text{mW m}^{-1} \text{K}^{-1}$) and was even better in thermal insulation than other materials

**Figure 5.** Thermal conductivity versus [NCO]/[OH] ratio of the PUR foams (data with different letters on the bar are significantly different, $P \leq 0.05$).

such as polyester fiber (about 35–43 $\text{mW m}^{-1} \text{K}^{-1}$) and cellular glass (about 36–55 $\text{mW m}^{-1} \text{K}^{-1}$), all of which are widely used in constructions for thermal insulation.¹³

It is reported that the k value of PUR foam was essentially decided by two factors, one of which is the direct conduction through the sequestered gas and PUR solid, whereas the other is the thermal radiation of the foam.¹⁴ Among them, thermal transfer of the gas sequestered inside the cells (CO_2 in this study) plays the most important role in determining the k value of a PUR foam (accounts for 60–65% of the overall k value).¹⁵ In addition, heat radiation and heat conduction by the cell structure contribute to the rest part of the k value. As cell size of the foams was very small, convection heat transfer inside the cells usually can be omitted.¹⁶

From Figure 5, it can be observed that Samples A–D showed no significant difference in the k values ($P \leq 0.05$). The cell size is supposed to have an effect on the k values. With a fixed apparent density, k value for the PUR foams would increase with decreasing cell size.¹⁷ However, such a result was not observed here. The possible reason is that the flat area between cells (noncellular part of PUR in the foam) is relatively large for the PUR foams in this study, as can be observed in Figure 1. The noncellular PUR segment is reported to have a much higher k value (220 $\text{mW m}^{-1} \text{K}^{-1}$) than the CO_2 (14.6 $\text{mW m}^{-1} \text{K}^{-1}$) sequestered inside the cells.³ Due to the excessive existence of the noncellular part of PUR, the effect of cell size was reduced significantly.

This argument can be further supported by Samples E and F, for which the k values increased significantly ($P \leq 0.05$; Figure 5). Such results should be ascribed to the increase in apparent density of both the samples, which caused an increase in the thermal conduction from the PUR solid. Though both Samples E and F showed satisfactory cell size distribution, quite a portion of the PUR solid of these samples was formed as the flat area but not the cells. For this reason, the thermal insulation provided by sequestered CO_2 could be weakened severely. In this study, the smaller “effective cellular volume” of our samples compared with the commercial insulation PUR foams caused the inferior thermal insulation of our samples compared with the commercial products. Further study should be focused on the improvement of the microstructure of the PUR foams, so as to achieve better thermal insulation.

DISCUSSION

Just like PUR foams made from bio-based polyols, cost is often the main constrain for the large-scale application of the foam.¹⁸ In this study, the most important cost is from HDI. One method to reduce the consumption of HDI is to lower the moisture content of the recycled ADF. However, dewatering through distillation in industrial scale is also an energy-intensive process. It is reported that energy requirements and cost increase significantly to concentrate glycol. Therefore, glycol should be concentrated only as much as necessary to meet the reuse application needs.¹⁹

In this study, the effect of moisture content of the recycled ADF was also studied. Distillation was used to decrease the moisture content of the recycled ADF to about 5.0 wt %, and then deion-

ized water was added to make different moisture contents of the recycled ADF as 10.0, 20.0, 30.0, and 40.0 wt %, respectively. $[\text{NCO}]/[\text{OH}]$ of 0.6 were used for all samples. Except for decreased HDI consumption due to lower moisture content of the recycled ADF, other components like PG, glycerin, and silicon oil were kept the same ratio as previous tests, whereas the usage of catalyst stannous octoate was reduced accordingly.

However, the recycled ADF with moisture content of 10.0, 20.0, and 30.0 wt % produced very poor structures after reaction, and the “free rising” process cannot be realized in such reactions. For the recycled ADF with moisture content of 40.0 wt %, the structure produced was relatively good, but still the free rising process was very limited compared with the previous tests of Sample C (with the same $[\text{NCO}]/[\text{OH}]$ ratio of 0.6 and moisture content of 51.6 wt %). The PUR foams produced from recycled ADF of 40% moisture content had a very high apparent density of $92.5 \pm 7.3 \text{ kg m}^{-3}$. The reason may be that the lower mass of water produced much less carbon dioxide during the reaction, which consequently restrained the foam rising process. For example, with the moisture content of 40.0 wt %, the water participating in the reaction accounted only for about 5.0 wt % of the total mass. Such a small quantity of water here could not produce enough carbon dioxide to sustain the free rising process, and bad structure resulted.

Also, the addition of glycerin would increase the cost in this study. It is reported that mixed-glycol streams are generally impractical to recycle due to the low market value of the resulting product, and perhaps only the deicing runoff from propylene glycol-based ADF/AAF is worthy of recovery, so as to ensure the highest value of the recycled material.¹⁹ However, it should be noted that for the propylene glycol- and glycerine-based ADF/AAF, the recycled runoff may be used directly to produce the PUR rigid foams.

For example, the aircraft deicing agent of SE/AMS 1424 type I from Octagon (Octagon Process, L.L.C., Las Vegas, Nevada) contains about 40–60 wt % propylene glycol, 40–60 wt % glycerin, as well as water (>10 wt %) and small amount of proprietary additives (<2 wt %; data provided by Octagon Process, L.L.C.). After recovery, the main component was 55 wt % water and about 45 wt % mixture of propylene glycol and glycerin (the trace amount of proprietary additives can be omitted after recycling). In this study, such recovered fluid was directly used for the production of PUR foams, and similar foams could be produced like the ones produced from the PG-based recycled ADF. Due to the already existence of glycerin in the recycled fluid, the addition of glycerin could be decreased greatly or even totally eliminated, which would help decrease the cost greatly. As it is difficult to determine the specific ratio between PG and glycerin in the recycled sample, systematic study was not conducted using this sample. However, further study is recommended to produce PUR foams from different kinds of recycled ADFs/AAFs, which will help find new ways to utilize such effluents economically.

CONCLUSIONS

PUR rigid foams were prepared from recycled ADF in this study. The effects of different $[\text{NCO}]/[\text{OH}]$ ratios on the

properties of the foams were determined. Generally, PUR foams from higher [NCO]/[OH] ratio displayed smaller cell size and better cell size distribution as well as higher compressive strength. Because of the contraction of the foam rising with [NCO]/[OH] ratio of 0.75 and 0.8, the apparent density increased significantly, resulting in increased thermal conductivity (k) as well as the sharp increase in the compressive strength. Due to the excessive existence of the noncellular PUR solid, the cell size showed little effect on k values, which were mainly controlled by apparent density. Recycled ADF with lower moisture content (10.0–40.0 wt %) were also tested in this study; however, poor structure was formed due to the low moisture content. In future, it is recommended to prepare PUR foams from different kinds of recycled ADFs/AAFs, which would help the management of such effluents in an economic way.

REFERENCES

1. Wu, J. P.; Wang, Y. H.; Wan, Y. Q.; Lei, H. W.; Yu, F.; Liu, Y. H.; Chen, P.; Yang, L. R.; Ruan, R. *Int. J. Agric. Biol. Eng.* **2009**, *2*, 40.
2. Zhang, L.; Jeon, H. K.; Malsam, J.; Herrington, R.; Macosko, C. W. *Polymer* **2007**, *48*, 6656.
3. Tan, S. Q.; Abraham, T.; Ference, D.; Macosko, C. W. *Polymer* **2011**, *52*, 2840.
4. Tu, Y.; Kiatsimkul, P.; Suppes, G.; Hsieh, F. *J. Appl. Polym. Sci.* **2007**, *105*, 453.
5. Narine, S. S.; Kong, X.; Bouzidi, L.; Sporn, P. *J. Am. Oil. Chem. Soc.* **2007**, *84*, 65.
6. Kurimoto, Y.; Takeda, M.; Koizumi, A.; Yamauchi, S.; Doi, S.; Tamura, Y. *Bioresour. Technol.* **2000**, *74*, 151.
7. Yu, F.; Le, Z. P.; Chen, P.; Liu, Y. H.; Lin, X. Y.; Ruan, R. *Appl. Biochem. Biotechnol.* **2008**, *148*, 235.
8. Switzenbaum, M. S.; Veltman, S.; Mericas, D.; Wagoner, B.; Schoenberg, T. *Chemosphere* **2001**, *43*, 1051.
9. United States Environmental Protection Agency (EPA Number: 821R00016). Preliminary Data Summary Airport Deicing Operations (revised), 2000, Section 10. Available at: <http://www.epa.gov/> (accessed August, **2011**).
10. United States Environmental Protection Agency (EPA Number: 821R00016). Preliminary Data Summary Airport Deicing Operations (revised), 2000, Section 6. Available at: <http://www.epa.gov/> (accessed August **2011**).
11. Gu, J. Y.; Gao, Z. H. *Sci. Technol. Eng.* **2003**, *5*, 462.
12. Huang, J.; Zhang, L. *Polymer* **2002**, *43*, 2287.
13. Energy Saving Trust (No. CE71). Insulation materials chart—thermal properties and environmental ratings, 2005. Available at: <http://www.energysavingtrust.org.uk/> (accessed August 2011).
14. Ahern, A.; Verbist, G.; Weaire, D.; Phelan, R.; Fleurent, H. *Colloid. Surf. A.* **2005**, *263*, 275.
15. Dohrn, R.; Fonseca, J. M.; Albers, R.; Kušan-Bindels, J.; Marrucho, I. M. *Fluid. Phase. Equilib.* **2007**, *261*, 41.
16. Gibson, L. J.; Ashby, M. F. Cellular Solids—Structure and Properties, 2nd ed.; Cambridge University Press: Cambridge, **1997**.
17. Bogdan, M.; Hoerter, J.; Moore, F. O. *J. Cell. Plast.* **2005**, *41*, 41.
18. Lu, Y.; Tighzert, L.; Dole, P.; Erre, D. *Polymer* **2005**, *46*, 9863.
19. Airport Cooperative Research Program (Report 14). Deicing planning guidelines and practices for stormwater management systems, 2009. Available at: <http://www.trb.org/ACRP/ACRP.aspx> (accessed August **2011**).